Queensland University of Technology
Brisbane Australia

This is the author's version of a work that was submitted/accepted for publication in the following source:

Njuguna, M.K., Yan, C., Hu, N., Bell, J.M., & Yarlagadda, P.K.D.V. (2012) Sandwiched carbon nanotube film as strain sensor. *Composites Part B : Engineering*, *43*(6), pp. 2711-2717.

This file was downloaded from: http://eprints.qut.edu.au/50628/

© Copyright 2012 Elsevier Ltd. All rights reserved.

This is the author's version of a work that was accepted for publication in <Composites Part B: Engineering>. Changes resulting from the publishing process, such as peer review, editing, corrections, structural formatting, and other quality control mechanisms may not be reflected in this document. Changes may have been made to this work since it was submitted for publication. A definitive version was subsequently published in Composites Part B: Engineering, [VOL 43, ISSUE 6, (2012)] DOI: 10.1016/j.compositesb.2012.04.022

Notice: *Changes introduced as a result of publishing processes such as copy-editing and formatting may not be reflected in this document. For a definitive version of this work, please refer to the published source:*

http://dx.doi.org/10.1016/j.compositesb.2012.04.022

Sandwiched carbon nanotube film as strain sensor

M. K. Njuguna[1], C. Yan[1]*, N. Hu[2], J.M. Bell[1], P.K. D. V. Yarlagadda[1]

[1]*School of Engineering Systems, Queensland University of Technology, 2 George St., GPO Box 2434, Brisbane, QLD 4000, Australia.*

[2]*Department of Mechanical Engineering, Chiba University, 1-33 Yayoi-cho, Inage-ku, Chiba 263-8522, Japan*

*Corresponding author:

Cheng Yan

School of Engineering Systems,

Queensland University of Technology, 2 George St. Brisbane, 40001, QLD,

Australia.

Email: c2.yan@qut.edu.au

Abstract

Two types of carbon nanotube nanocomposite strain sensors were prepared by mixing carbon nanotubes with epoxy (nanocomposite sensor) and sandwiching a carbon nanotube film between two epoxy layers (sandwich sensor). The conductivity, response and sensitivity to static and dynamic mechanical strains in these sensors were investigated. The nanocomposite sensor with 2~3% wt carbon nanotube demonstrated high sensitivity to mechanical strain and environmental temperature, with gauge factors of 5~8. On the other hand, a linear relationship between conductivity and dynamic mechanical strain was observed in the sandwich sensor. The sandwich sensor was also not sensitive to temperature although its strain sensitivity (gauge factor of about 3) was lower as compared with the nanocomposite sensor. Both sensors have excellent response to static and dynamic strains, thereby having great potential for strain sensing applications.

Keywords: A. Smart materials; A. Nano-structures A. Polymer-matrix composites B. Electrical properties;

1. Introduction

Carbon nanotubes (CNTs) have excellent electrical, mechanical and electromechanical properties. When CNTs are incorporated into polymers, nanocomposites with high electrical conductivity at very low CNT contents can be produced. For instance, conductivities in the order of 10^{-1} S/m can be easily achieved with less than 0.5%wt CNT [1-3]. In addition, the conductivity of these nanocomposites changes with mechanical strain, providing a possibility for development of novel strain or damage sensors. There are several ways to make CNT based strain or damage sensors. For example, individual CNTs can be mixed with polymer to create composite sensors [4-8], integrated into other micro-systems such as micro electromechanical systems (MEMS) [9], processed to form CNT films [10] *and added into fibre reinforced composites to make smart materials [11-13]*.

In general, nanocomposite type strain sensors have high strain sensitivity, with up to 10 times the gauge factor of traditional metal foil strain gauges [9, 14-17]. The relationship between conductivity and applied strain is generally linear under small strains ($\leq 1000\mu\varepsilon$) [18]. The highest sensitivity in composite type sensor is obtained near the percolation threshold due to the tunnelling effect between adjacent CNTs and decreases with further increase of carbon nanotube loading [4, 17, 18]. This makes the performance of composite sensors highly dependent on processing conditions and material properties such as CNT volume fraction and conductance, curing temperature, mixing rate and barrier height of polymer matrix [4, 19]. To some extent, the overall performance can be

dominated by matrix properties rather than the intrinsic characteristics of CNTs. For instance, nonlinear sensor response under large strains has been observed [4, 19]. Therefore, it is necessary to develop novel sensors to reduce the possible impact from polymer matrix and take the advantage of the intrinsic properties of CNTs. On the other hand, CNT film sensors have demonstrated good response to mechanical strains and offered the possibility of multidirectional and multi-point sensing [10]. Unfortunately, their electrical characteristics are not stable due to the weak bonding between the CNTs and polymer via van der Waals attraction. In addition, these CNT films are extremely fragile and difficult to be used for practical applications. In addition, the influence of environmental factors such as temperature on the performance of CNT based strain sensors has not been well understood.

In this work, we developed a new type CNT- polymer strain sensor by sandwiching a CNT film within polymer layers. Its electrical properties and strain sensing performance was investigated and compared with composite type sensors. Some useful conclusions were achieved in relation to temperature effect, strain sensitivity and sensing performance under both static and dynamic loads.

2. Experiment

2.1 Materials

Chemical vapour deposition (CVD) synthesized multiwall carbon nanotubes (MWCNTs, Nano Carbon Technologies Corporation, Tokyo, Japan) with purity of higher than 99.5% were used. The typical diameter and length of

the pristine MWCNTs are in the range of 33~124 nm (70 nm in average) and 1.1 to 22.5 μm (average: 8.7 μm) respectively. The epoxy resin system was Araldite® GY191 cured with Aradur HY956. Both resin and hardener were supplied by CG Composites, Brisbane, Australia. Araldite® GY191 is predominantly diglycidyl ether of Bisphenol A (DGEBA), with Bisphenol-F epoxy resin and glycidyl ethers of C_{12}-C_{14} alcohols as minor components. Aradur HY956 is a low viscosity polyamine (triethylenetetramine (*TETA*)) hardener.

2.2 Sensor preparation

The first type of sensor was made by sandwiching a CNT film between two epoxy layers. The epoxy layers were used to protect the CNT film that is generally fragile. 25 mg of carbon nanotube was dispersed in 50 ml of dimethylformamide (DMF) using bath sonication for 30 min. Low power bath sonication was employed to avoid possible damage to the carbon nanotubes. The carbon nanotube film was obtained by filtering the DMF solution using a membrane filter. The residual DMF was washed away from the film using deionised water, followed by drying at 80^{o}C for 12h. Optical and scanning electron microscopy (SEM) images of the dry CNT film are shown in Fig. 1 (a) and (b) respectively. To fabricate the sandwich film sensor, epoxy-TETA mixture (4:1) was prepared and applied on an aluminium plate. The CNT film was peeled off from the filter and placed on the epoxy-hardener mixture. Liquid epoxy was then spread on the top surface of the CNT film. The sandwiched sample was cured at room temperature for 24 h under a pressure of 0.5MPa to ensure a

uniform spread of the epoxy on the CNT film. The SEM image shown in Fig. 1 (c) reveals a CNT rich region covered with an epoxy layer. Fig. 1 (d) shows the sandwich sensor mounted on a brass substrate. The sandwich sensor had a thickness of ~120 μm. The sandwich structure is schematically illustrated in Fig. 2 (a)

The second type of sensor was prepared by dispersing up to 3% wt. CNT in epoxy using a planetary shear mixer. *In general, two methods commonly used to disperse CNTs in epoxy, i.e., (a) shear mixing, and (b) dispersion of nanotubes in a solvent (acetone) and then in epoxy using sonication. Shear mixing was selected in this work because sonication has the potential to cause structural damage to the CNTs, causing degradation of their electrical properties. In addition, good dispersion has been achieved in the composites with the same CNT using the shear mixing method alone [2, 20]*. First, epoxy resin and curing agent in a ratio of 4:1 was mixed for 30 s. Then the MWCNT was added and further mixed for 60 s with a mixing speed of 2000 rpm. The epoxy/CNT nanocomposite films with thickness ~150 μm were obtained by tape casting on glass slides and cured for 24 h at room temperature. *The weight fraction of three sandwich sensor samples as determined by thermogravimetric analysis (TGA) was 42.3±3.6 wt. %.* The process is schematically shown in Fig. 2 (b). Hereafter, we refer to these two types of sensors as sandwich and composite sensors, respectively.

2.3 Evaluation of electrical properties and sensing performance

The prepared sensors were cut into sheet samples (12x6 mm) for evaluation of the electrical properties and the sensing performance. Electrical resistance was measured using a digital multimeter (Agilent 34401A). The static strain sensing characteristics were evaluated in static tension. To examine the

response to dynamic strains, the sensors were attached to a cantilever beam and sinusoidal loads with different amplitudes and frequencies were applied to the beam via a shaker. The output signal from the sensors was recorded, processed and collected using a bridge circuit, bridge box and an oscilloscope respectively. The experimental set up for dynamic strain sensing is schematically shown in Fig. 3. The relationship between the bridge output voltage E and the bridge input voltage V is expressed as [21],

$$E = \frac{V}{4} K\varepsilon \tag{1}$$

where K is the gauge factor and ε the applied strain. The gauge factor measures the sensitivity of the strain sensor and is expressed as the ratio of relative change in resistance to applied strain, i.e.,

$$K = \frac{\Delta R / R_o}{\varepsilon} \tag{2}$$

Using equations 1 and 2, the resistance change can be expressed as,

$$\frac{\Delta R}{R_o} = \frac{4E}{V} \tag{3}$$

where ΔR is the change in resistance and R_o is original resistance. Equation 3 was used to evaluate the relative resistance change in these sensors.

To examine the temperature effect on resistivity, the sensors were placed in an environment chamber with humidity 63.1% and temperature varying between -20^{o}C and 50^{o}C at a heating and cooling rate of 2.5^{o}C/min.

3. Results and Discussion

3.1 Conductivity and temperature sensitivity

The variation of conductivity in the nanocomposites with MWCNT loading is shown in Fig. 4. It is clear that the addition of CNT into the polymer resin significantly increases the conductivity (~2 $\times$ 10^{-14} S/m in epoxy resin [22]) by up to 10-12 orders of magnitude. In general, the conductivity in a composite system above percolation threshold can be described by the following scaling law [23]:

$$\sigma = \sigma_o(\theta - \theta_c)^t \qquad (4)$$

where θ is the volume or weight fraction of the conducting filler, θ_c is the percolation threshold and t is the critical exponent. Curve fitting of the experimental data in Fig. 4 gives t = 2.4 ± 0.51 and percolation threshold θ_c = 0.5 ± 0.05. These values are similar to the values observed in other CNT/epoxy nanocomposites [24].

The sensitivity to environmental temperature in the nanocomposite and sandwich sensors was evaluated. *The glass transition temperatures (T_g) of both the 2 and 3% wt. CNT nanocomposites, determined using differential scanning*

calorimetry (DSC) was 71^{o}C, hence for the maximum temperature used in this study was set at 50^{o}C. Low temperature sensitivity is generally preferred for practical strain sensing. As shown in Fig. 5, when temperature increases from -20 to 50^{o}C, the resistivity in the nanocomposite sensors with 2% and 3% wt. CNT changes up to 140% and 35%, respectively**.** On the other hand, only 2.5% change in the resistivity was observed in the sandwich sensor. For simplicity, the 2% wt. CNT, 3% wt. CNT composite and sandwich sensors are referred to as EP2, EP3 and SW, respectively. For comparison, standard strain gauge was also evaluated and negligible resistivity change was observed in the temperature range tested. Therefore, the EP2 and EP3 sensors have higher temperature sensitivity as compared to the SW sensor. Li *et al*. [10] reported a slight drop of resistance (0.1Ω) in a pristine MWCNT film over the temperature range 273-363 K, indicating a temperature independent resistance response. Other studies reported a similar resistance - temperature response in pristine MWCNT films in the temperature range of 100-430 K [25] and 123-573 K [26]. The similarity between these reports on pristine MWCNT films and the result shown in Fig. 5 indicates that the polymer layers on the top and bottom of the MWCNT film in the SW sensors do not influence its electrical properties. In other words, the carbon nanotube networks formed within the film largely dominate the resistance - temperature response. In this case, the total resistance of the nanotube film (R_f) can be assumed to be the sum of individual carbon nanotube resistance, R_{cnt} and the nanotube-nanotube junction resistance R_j, i.e.,

$$R_f = R_j + R_{cnt} \quad (5)$$

The temperature response from the CNTs can then be described using a modified Luttinger liquid model [27], by which the resistance change is correlated with the temperature in the form of $R(T) = R_{cnt}T^{-\alpha}$, where α is a constant. On the other hand, the resistance - temperature response contributed by the CNT junctions can be modelled using Fermi liquid model, i.e., $R(T) = R_jT$ [27]. In this model, the Luttinger component recognises the interaction of electrons in the carbon nanotubes as one-dimensional conductors. The Fermi liquid component is included to model the interaction of electrons at the CNT junctions, where the Luttinger component is expected to break down, and the CNT junctions can be considered as metal-metal junctions [27]. As a result, the conductive network within a CNT film in the sandwich sensor is considered as a series of resistors, as shown schematically in Fig. 6. The total resistance as a function of temperature can be expressed as,

$$R(T) = R_{cnt}T^{-\alpha} + R_jT \quad (6)$$

As shown in Fig. 7, equation 6 fits the experimental data very well, with α = 0.14. The reported α values corresponding to individual MWCNTs and a mat consisting of MWCNTs are in the range of 0.36~0.95 [28] and 0.22 [27], respectively. The value for the sandwich sensor, i.e., 0.14 is close to the value corresponding to the MWCNT mat.

As shown in Fig. 5, the nanocomposite sensors are more sensitive to environmental temperature. Compared to the SW sensor, this temperature dependent resistivity is believed to be the influence of the polymer matrix. The thermal expansion coefficient of epoxy is about $7.5 \times 10^{-5}\ K^{-1}$[22]. On the other hand, the thermal expansion of MWCNTs is in the range $0.73 - 1.49 \times 10^{-5}\ K^{-1}$ [29]. Around the percolation threshold, it has been confirmed that the resistivity of CNT-polymer composites is dominated by tunnelling between neighbouring CNTs [19]. The difference in CTEs between nanotubes and epoxy may lead to significant change in the tunnelling distance as the epoxy phase expands and contracts during the heating and cooling cycles. When temperature increases, the inter-tubes distance in the CNT network is increased, resulting in increase of resistance. A reverse process occurs during cooling.

In summary, the resistance in EP2 and EP3 composite sensors is highly sensitive to temperature but the resistance in the SW sensor is almost independent of temperature. In the composite sensors, the CNT surface is often coated with a thin layer of polymer, which prevents the direct connection of neighbouring MWCNTs, as shown in Fig. 1 (d). This has been confirmed by the atomic force microscopy (AFM) observation on the plasma etched CNT-epoxy composites [30]. The distance between neighbouring nanotubes increases with temperature due to the expansion of polymer. This leads to an increase in the tunneling resistance, which is responsible for the higher temperature sensitivity. As expected, the sensitivity to temperature decreases with increasing the MWCNT

loading, as shown in Fig. 5. For the sandwich sensors, as illustrated by Equation 6 and 7, the temperature response is dominated by the resistivity of nanotubes and nanotube-nanotube junctions. The conductive networks were formed in the CNT through the direct connection of individual CNTs. The polymer layers coated on the top and bottom of the CNT film do not significantly interfere with the CNT networks formed. This leads to lower temperature sensitivity in the sandwich sensors. The low temperature sensitivity observed in the sandwich sensor is a significant advantage for practical applications.

3.2 Piezoresistivity under static loading

The change of resistance in the sensors as a function of strain (piezoresistivity) is shown in Fig. 8. Three samples were tested in each case. A linear tensile strain - resistance response was observed in both the nanocomposite and sandwich sensors. For strain sensing, a high sensitivity to applied strain is desirable. The sensitivity is generally estimated by gauge factor (K) which relates the change in resistance to the external strain ε. This relationship is shown in Equation 2. As shown in Fig. 8, EP2 has the highest gauge factor (8.54), followed by EP3 (5.31), and SW (2.99). The gauge factor of a conventional metal foil strain gauge is 2. As compared to the composite sensors, the increased contact of the individual CNTs in the sandwich sensor may reduce the tunnelling effect between neighbouring CNTs, causing reduced strain sensitivity. *In Fig. 8, there is a slight 'slope drop' in the resistivity curve corresponding to about 450 με. This slope*

drop may be associated with rearrangement of the CNT network with increase in strain.

Depending on fabrication process, carbon nanotube and polymer matrix, a range of gauge factors have been reported in literature [4, 17, 18]. In general, increase of carbon nanotube content in a composite leads to a decrease of gauge factor. This has been confirmed in this work as a higher gauge factor is associated with the composites sensor with 2% CNT (EP2). It is clear that the gauge factor of the sandwich sensor is lower than the composite sensor but still higher than conventional strain gauge. Another advantage of the sandwich sensor is the lower sensitivity to environmental temperature as discussed above.

3.3 Dynamic strain sensing

The relative resistance change in the sensors attached to a cantilever beam subjected to dynamic loading at different frequencies and amplitudes can be also evaluated using Equation 3. *Figures 9 (a) – (c) show the response from all sensors at 100 Hz. The* loading cycles were accurately detected and recorded by the SW and the composite sensors. Obviously, the signal strength is different in the sensors. The highest amplitude of $\Delta R/R_o$ is associated with the 2% CNT composite sensor due to its high gauge factor. Similar response was observed in these sensors corresponding to other frequencies (50 and 200 Hz).

The relative resistance change ($\Delta R/R_o$) in the sandwich sensor against tension and compression dynamic strains at 100Hz is shown in Fig. 10. A

repeatable linear response to both tension and compression dynamic strains can be observed. In addition, the response is approximately symmetric about the origin. The linear fit through the origin in Fig. 10 gives an average slope of 3.13, which is close to the gauge factor of 2.99 obtained in the static tensile test.

The variation of $\Delta R/R_o$ with dynamic strain in the conventional metallic strain gauge for sandwich and composite sensors was recorded at different frequencies (50 and 100 Hz), as shown in Fig. 11 (a) and (b). It is clear that a linear relationship exhibits between $\Delta R/R_o$ and strain in the sandwich sensor and the composite sensor with 3% CNT. Corresponding to the same strain, $\Delta R/R_o$ increases with decreasing the frequency in all sensors, especially in the sandwich and composite sensor with 3% CNT. The composite sensor with 2% CNT demonstrates a higher $\Delta R/R_o$ at the same strain level, as compared to the other sensors. This is attributed to the higher gauge factor (high strain sensitivity) in the composite sensor with 2% CNT, consistent with its performance under static loading.

4. Conclusions

Two types of CNT based strain sensors were developed by inserting a CNT film between two epoxy layers (sandwich sensor) and dispersing small amount (2-3%) of CNT into epoxy (composite sensor). Based on the evaluation of electrical properties and sensing performance in these sensors, we found that the resistance of the sandwich sensor is insensitive to environmental temperature but temperature dependent resistance was observed in the composite sensors,

especially the one with 2% CNT. All sensors demonstrate excellent response to both static and dynamic loads. As compared to conventional strain gauge, higher strain sensitivity (gauge factor) is observed in these sensors, in particular the composite sensor with 2% CNT. A symmetric response to tension and compression loads is also observed in the sandwich sensor. The resistivity of the sandwich sensor is mainly contributed by the intrinsic resistivity of CNT and the CNT junctions, and its dependence with temperature can be described by a modified Luttinger liquid model.

References

[1] A. Moisala, Q. Li, I.A. Kinloch, A.H. Windle, Thermal and electrical conductivity of single- and multi-walled carbon nanotube-epoxy composites, Composites Science and Technology, 66 (2006) 1285-1288.

[2] N. Hu, Z. Masuda, C. Yan, G. Yamamoto, H. Fukunaga, T. Hashida, The electrical properties of polymer nanocomposites with carbon nanotube fillers, Nanotechnology, 19 (2008) 215701.

[3] J. Sandler, M.S.P. Shaffer, T. Prasse, W. Bauhofer, K. Schulte, A.H. Windle, Development of a dispersion process for carbon nanotubes in an epoxy matrix and the resulting electrical properties, Polymer, 40 (1999) 5967-5971.

[4] N. Hu, Y. Karube, M. Arai, T. Watanabe, C. Yan, Y. Li, Y. Liu, H. Fukunaga, Investigation on sensitivity of a polymer/carbon nanotube composite strain sensor, Carbon, 48 (2010) 680-687.

[5] G. Yin, N. Hu, Y. Karube, Y. Liu, Y. Li, H. Fukunaga, A carbon nanotube/polymer strain sensor with linear and anti-symmetric piezoresistivity, Journal of Composite Materials, (2011) 1-8.

[6] S. Deshmukh, Z. Ounaies, Single walled carbon nanotube (SWNT)-polyimide nanocomposites as electrostrictive materials, Sensors and Actuators A: Physical, 155 (2009) 246-252.

[7] X. Yu, R. Rajamani, K. Stelson, T. Cui, Carbon nanotube-based transparent thin film acoustic actuators and sensors, Sensors and Actuators A: Physical, 132 (2006) 626-631.

[8] A.K.T. Lau, D. Hui, The revolutionary creation of new advanced materials—carbon nanotube composites, Composites Part B: Engineering, 33 (2002) 263-277.

[9] C. Neng-Kai, S. Chi-Chung, C. Shuo-Hung, Fabrication of single-walled carbon nanotube flexible strain sensors with high sensitivity, Applied Physics Letters, 92 (2008) 063501-063501.

[10] X. Li, C. Levy, L. Elaadil, Multiwalled carbon nanotube film for strain sensing, Nanotechnology, 19 (2008) 045501-045501.

[11] L. Gao, T.W. Chou, E.T. Thostenson, Z. Zhang, M. Coulaud, In situ sensing of impact damage in epoxy/glass fiber composites using percolating carbon nanotube networks, Carbon, 49 (2011) 3371-3391.

[12] S.M. Friedrich, A.S. Wu, E.T. Thostenson, T.W. Chou, Damage mode characterization of mechanically fastened composite joints using carbon nanotube networks, Composites Part A: Applied Science and Manufacturing, (2011) 2003-2009.

[13] A.S. Lim, Z.R. Melrose, E.T. Thostenson, T.W. Chou, Damage sensing of adhesively-bonded hybrid composite/steel joints using carbon nanotubes, Composites Science and Technology, 71 (2011) 1183-1189.

[14] C. Stampfer, T. Helbling, D. Obergfell, B. Schöberle, M. Tripp, A. Jungen, S. Roth, V. Bright, C. Hierold, Fabrication of single-walled carbon-nanotube-based pressure sensors, Nano Letters, 6 (2006) 233-237.

[15] C.L. Wu, H.C. Lin, J.S. Hsu, M.C. Yip, W. Fang, Static and dynamic mechanical properties of polydimethylsiloxane/carbon nanotube nanocomposites, Thin Solid Films, 517 (2009) 4895-4901.

[16] R. Zhang, M. Baxendale, T. Peijs, Universal resistivity–strain dependence of carbon nanotube/polymer composites, Physical Review B, 76 (2007) 195433.

[17] I. Kang, M.J. Schulz, J.H. Kim, V. Shanov, D. Shi, A carbon nanotube strain sensor for structural health monitoring, Smart Materials and Structures, 15 (2006) 737-748.

[18] Giang T. Pham, Young-Bin Park, Zhiyong Liang, Chuck Zhang, Ben Wang, Processing and modeling of conductive thermoplastic/carbon nanotube films for strain sensing, Composites Part B: Engineering, 39 (2008) 209-216.

[19] N. Hu, Y. Karube, C. Yan, Z. Masuda, H. Fukunaga, Tunneling effect in a polymer/carbon nanotube nanocomposite strain sensor, Acta Materialia, 56 (2008) 2929-2936.

[20] N. Hu, Z. Masuda, G. Yamamoto, H. Fukunaga, T. Hashida, J. Qiu, Effect of fabrication process on electrical properties of polymer/multi-wall carbon nanotube nanocomposites, Composites Part A: Applied Science and Manufacturing, 39 (2008) 893-903.

[21] Yokogawa, {DL750/DL750P ScopeCorder User's Manual}, in, Yokogawa Electric Organization, 2006, pp. 78-98.

[22] Materials Data Sheet, Araldite GY191, in, Huntsman Corporation, 2006.

[23] D. Stauffer, Introduction to Percolation Theory, Taylor and Francis, London, 1985.

[24] W. Bauhofer, J.Z. Kovacs, A review and analysis of electrical percolation in carbon nanotube polymer composites, Composites Science and Technology, 69 (2009) 1486-1498.

[25] D. Mendoza, Electrical properties of carbon nanofibers synthesized using carbon disulfide as precursor, Optical Materials, 29 (2006) 122-125.

[26] N. Koratkar, A. Modi, E. Lass, P. Ajayan, Temperature effects on resistance of aligned multiwalled carbon nanotube films, Journal of nanoscience and nanotechnology, 4 (2004) 744-748.

[27] D.J. Bae, K.S. Kim, Y.S. Park, E.K. Suh, K.H. An, J.M. Moon, S.C. Lim, S.H. Park, Y.H. Jeong, Y.H. Lee, Transport phenomena in an anisotropically aligned single-wall carbon nanotube film, Physical Review B, 64 (2001) 233401.

[28] E. Graugnard, P. De Pablo, B. Walsh, A. Ghosh, S. Datta, R. Reifenberger, Temperature dependence of the conductance of multiwalled carbon nanotubes, Physical Review B, 64 (2001) 125407.

[29] F. Wu, H. Cheng, Structure and thermal expansion of multi-walled carbon nanotubes before and after high temperature treatment, Journal of Physics D: Applied Physics, 38 (2005) 4302.

[30] M.K. Njuguna, C. Yan, J.M. Bell, K.D.V. Yarlagadda, Microscale study of electrical characteristics of multi wall carbon nanotube/epoxy nanocomposites, in:

6th IEEE International Conference on Nano/Micro Engineered and Molecular Systems, Kaohsiung, Taiwan, 2011, pp. 525 - 528.

Figure Captions

Figure 1. (a) Dry CNT film, (b) SEM image of CNT film before coating with polymer, (c) SEM image of a cross section of the sandwich film, and (d) composite with 3% wt. CNTs.

Figure 2. Schematic of (a) structure of a sandwich sensor, (b) fabrication process of composite sensor, and (c) sensor mounted on a tensile test specimen

Figure 3. Schematic of the experimental setup for dynamic strain sensing

Figure 4. Change of conductivity with CNT loading in composite.

Figure 5. Temperature versus relative resistance change in SW, EP2 and EP3 sensors, and metallic foil strain gauge.

Figure 6. A schematic diagram of CNT-CNT junctions showing the resistance of sandwich sensor.

Figure 7. Plot of R (T)/T against temperature for the sandwich film. The continuous line is the fit to the experimental data using modified Luttinger model.

Figure 8. Piezoresistivity of sandwich sensor, composite sensors with 2 and 3% CNT, and strain gauge at 25^{o}C.

Figure 9. Relative resistance change in (a) sandwich sensor, (b) EP2 sensor, (c) EP3 sensor under dynamic strain at 100Hz.

Figure 10. Relative resistance change with dynamic strain in the sandwich sensor at 100Hz.

Figure 11. Peak to peak relative resistance change against strain for sandwich sensor, composite with 2 and 3% CNT at (a) 100Hz and (b) 50Hz.

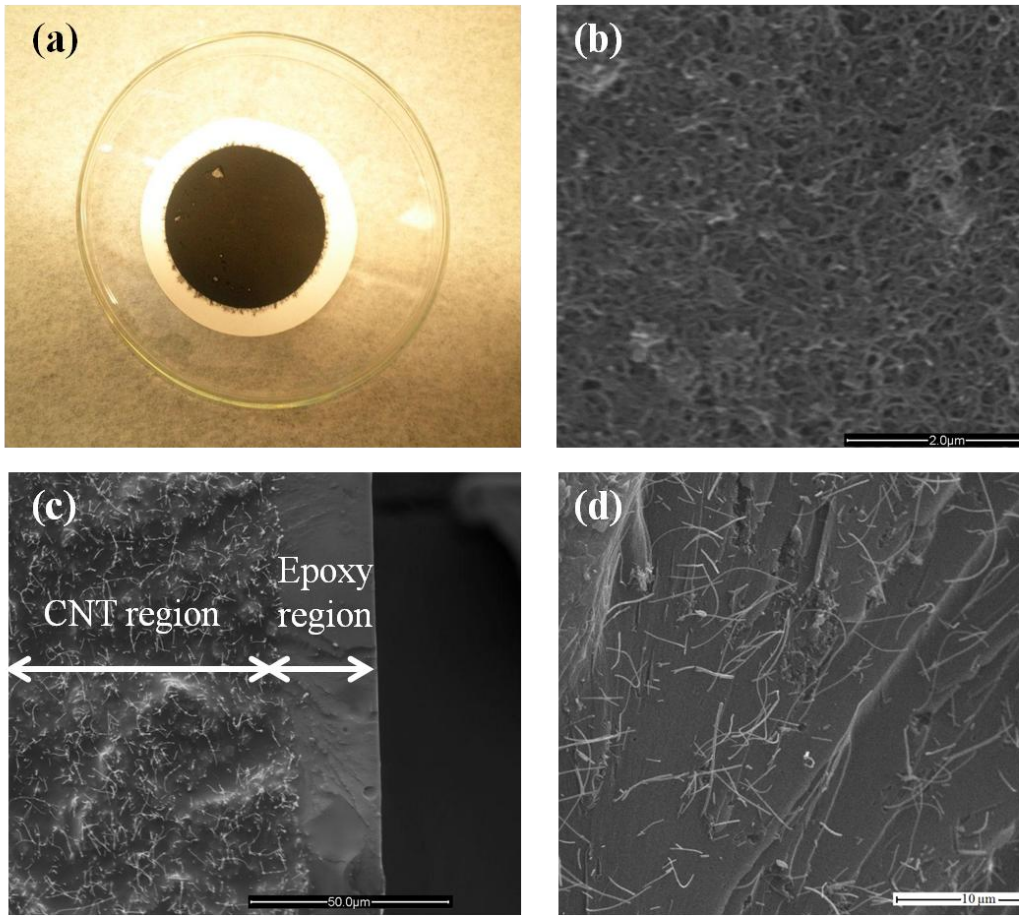

Figure 1.

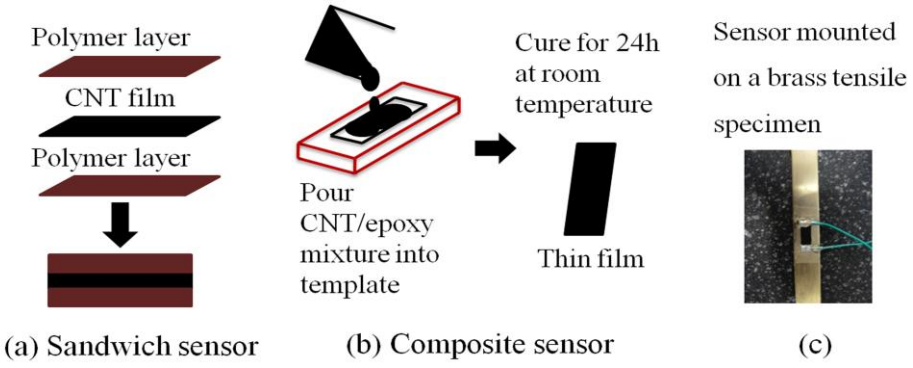
Polymer layer
CNT film
Polymer layer
Pour CNT/epoxy mixture into template
Cure for 24h at room temperature
Thin film
Sensor mounted on a brass tensile specimen
(a) Sandwich sensor
(b) Composite sensor
(c)

Figure 2

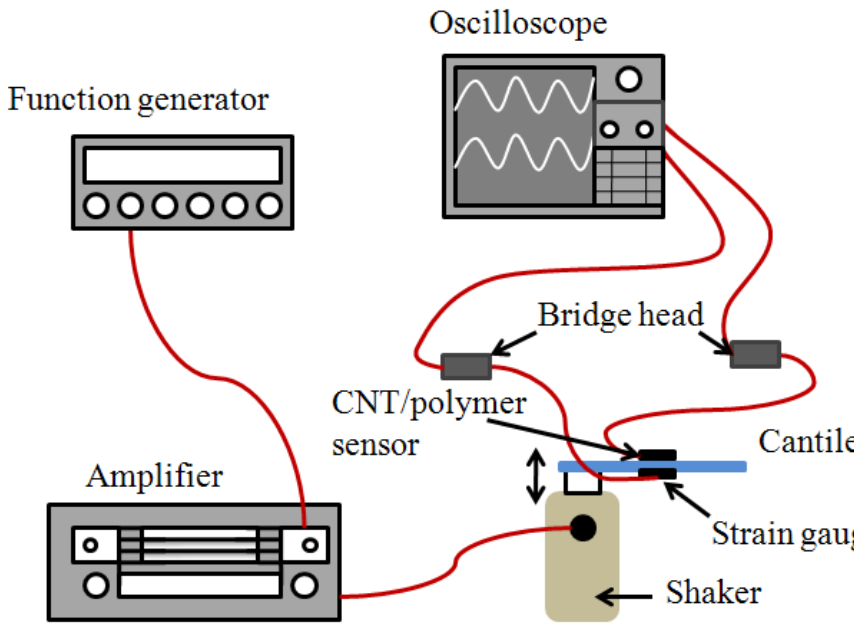
Oscilloscope
Function generator
Bridge head
CNT/polymer
sensor
Cantile
Amplifier
Strain gau
Shaker

Figure 3

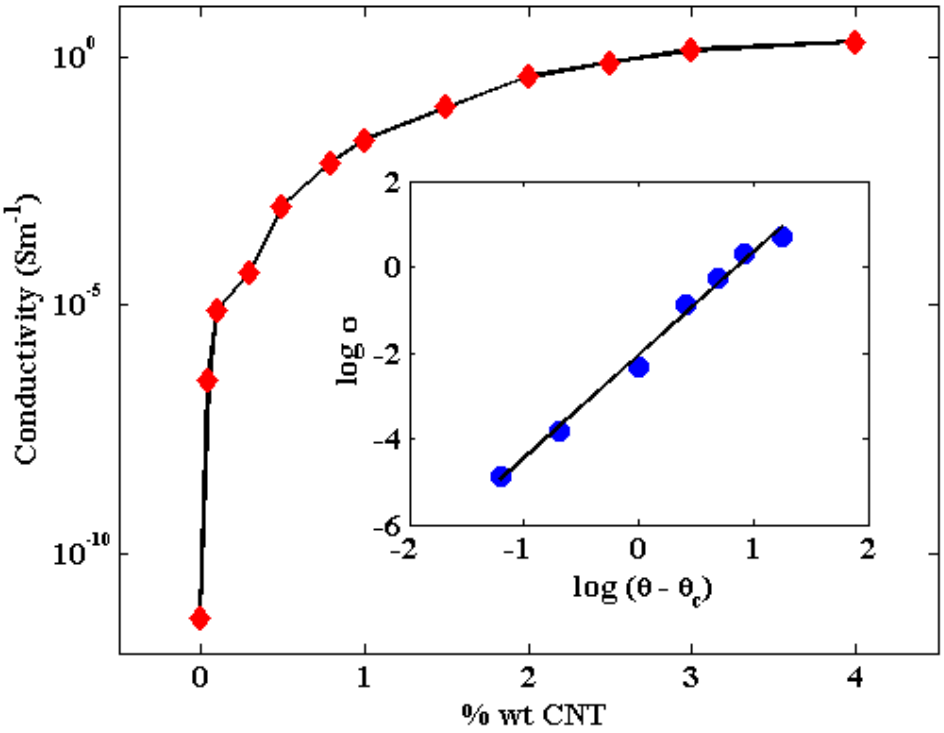
Conductivity (Sm-1)
10^0
10^-5
10^-10
0
1
2
3
4
% wt CNT
log σ
2
0
-2
-4
-6
-2
-1
0
1
2
log (θ - θc)

Figure 4

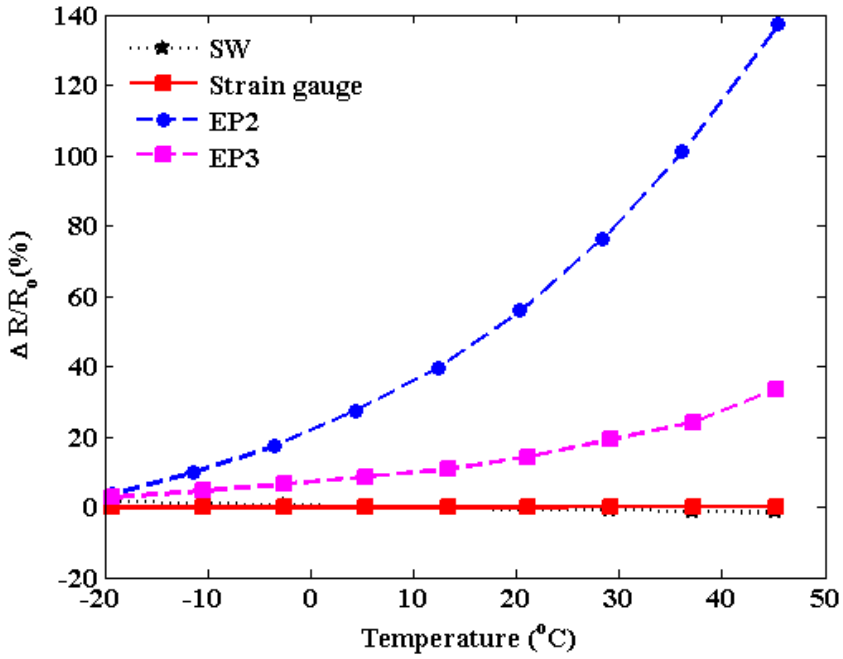
SW
Strain gauge
EP2
EP3
ΔR/R0 (%)
Temperature (°C)
140
120
100
80
60
40
20
0
-20
-20
-10
0
10
20
30
40
50

Figure 5

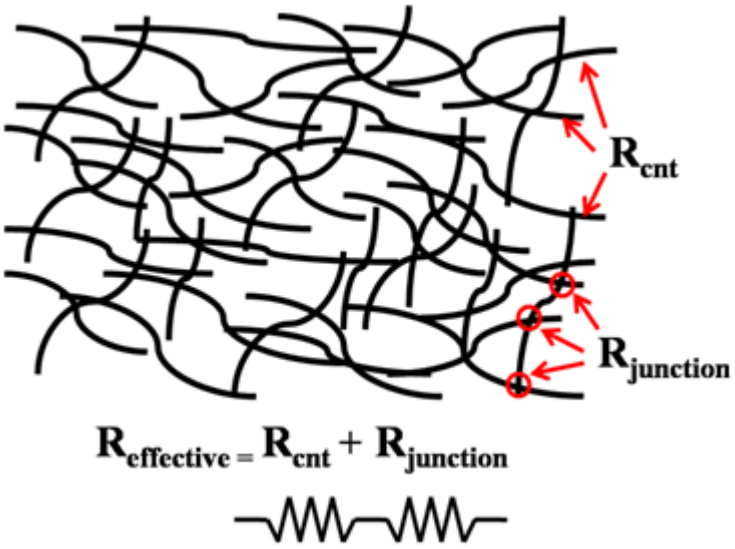

Figure 6:

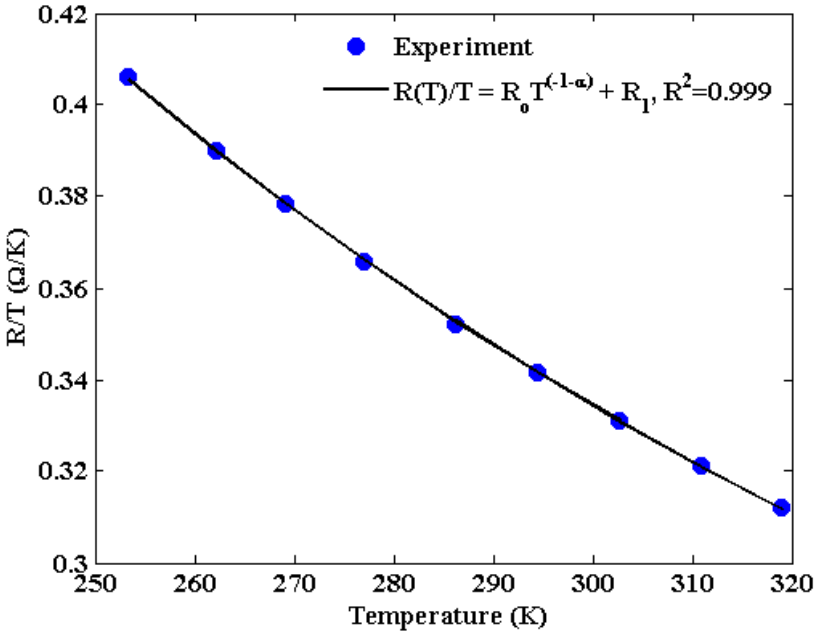
Experiment
R(T)/T = R0 T^(-1-α) + R1, R^2=0.999
R/T (Ω/K)
Temperature (K)
0.42
0.4
0.38
0.36
0.34
0.32
0.3
250
260
270
280
290
300
310
320

Figure 7

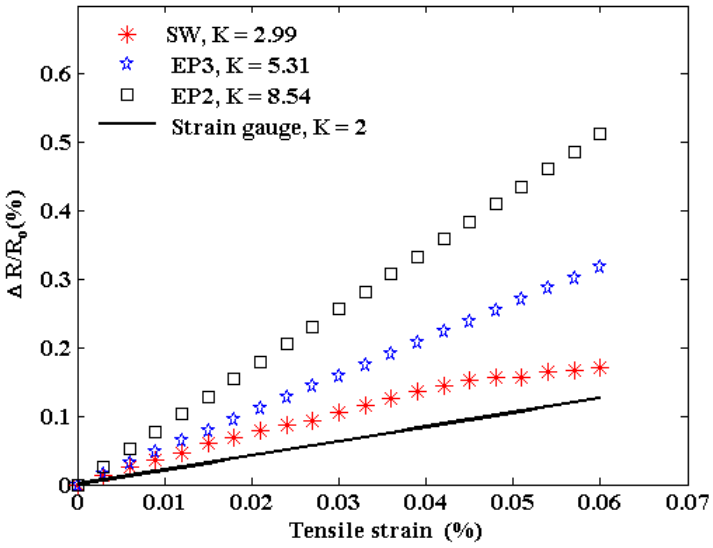
SW, K = 2.99
EP3, K = 5.31
EP2, K = 8.54
Strain gauge, K = 2
Δ R/R0 (%)
Tensile strain (%)
0
0.1
0.2
0.3
0.4
0.5
0.6
0.01
0.02
0.03
0.04
0.05
0.06
0.07

Figure 8

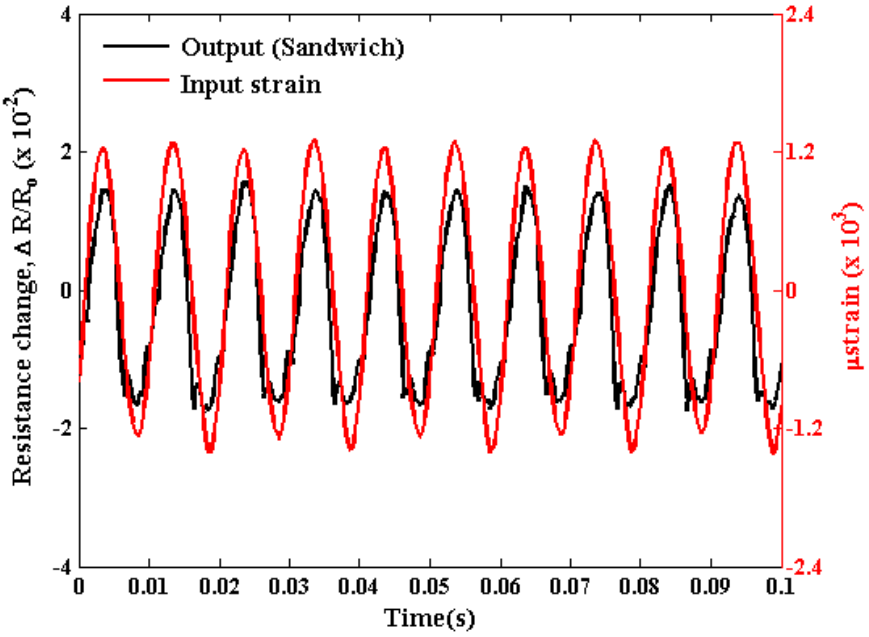
Output (Sandwich)
Input strain
Resistance change, Δ R/R$_o$ (x 10^{-2})
μstrain (x 10^3)
Time(s)
4
2
0
-2
-4
2.4
1.2
0
-1.2
-2.4
0
0.01
0.02
0.03
0.04
0.05
0.06
0.07
0.08
0.09
0.1

Figure 9 (a)

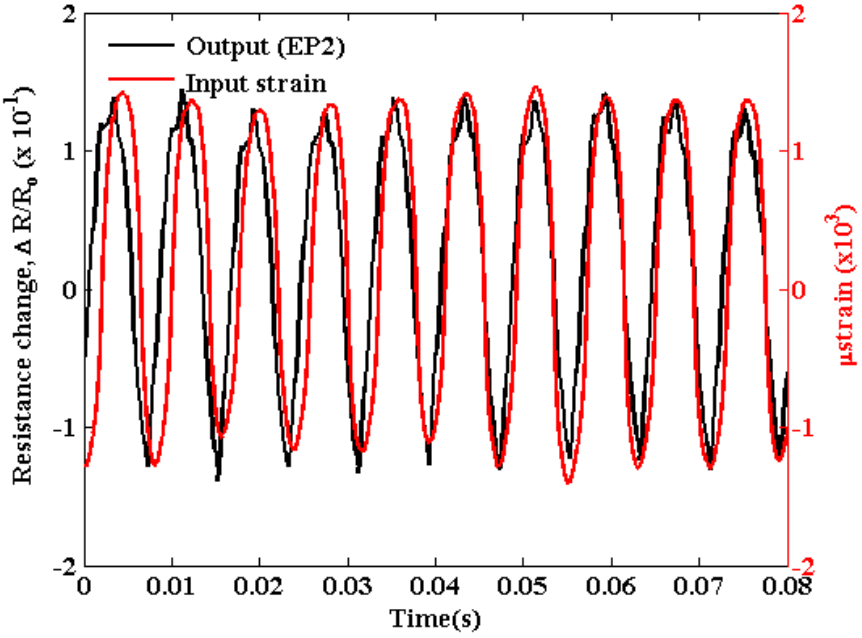
Output (EP2)
Input strain
Resistance change, Δ R/R$_o$ (x 10^{-1})
μstrain (x10^3)
Time(s)
2
1
0
-1
-2
0
0.01
0.02
0.03
0.04
0.05
0.06
0.07
0.08

Figure 9 (b)

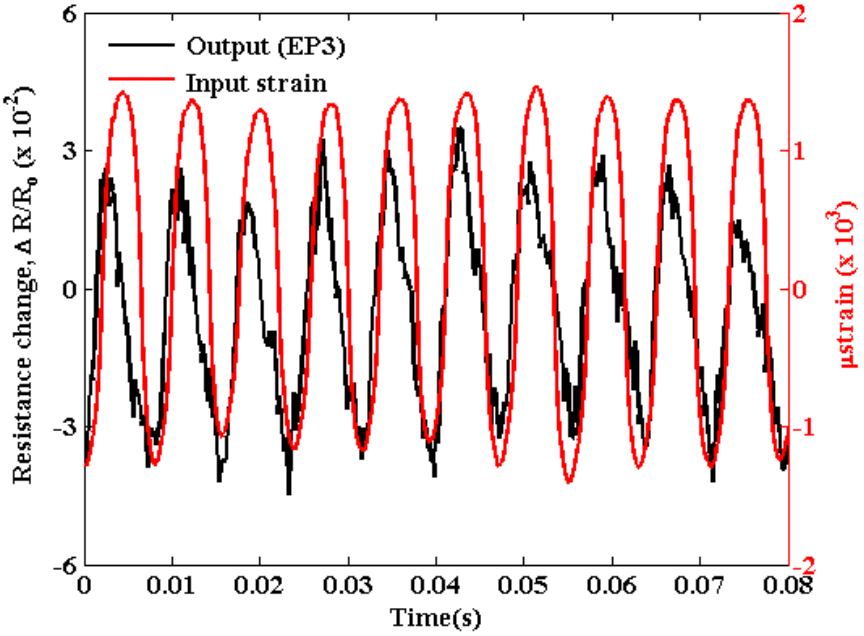
Output (EP3)
Input strain
Resistance change, Δ R/R$_0$ (x 10^{-2})
μstrain (x 10^3)
Time(s)
6
3
0
-3
-6
2
1
0
-1
-2
0
0.01
0.02
0.03
0.04
0.05
0.06
0.07
0.08

Figure 9 (c)

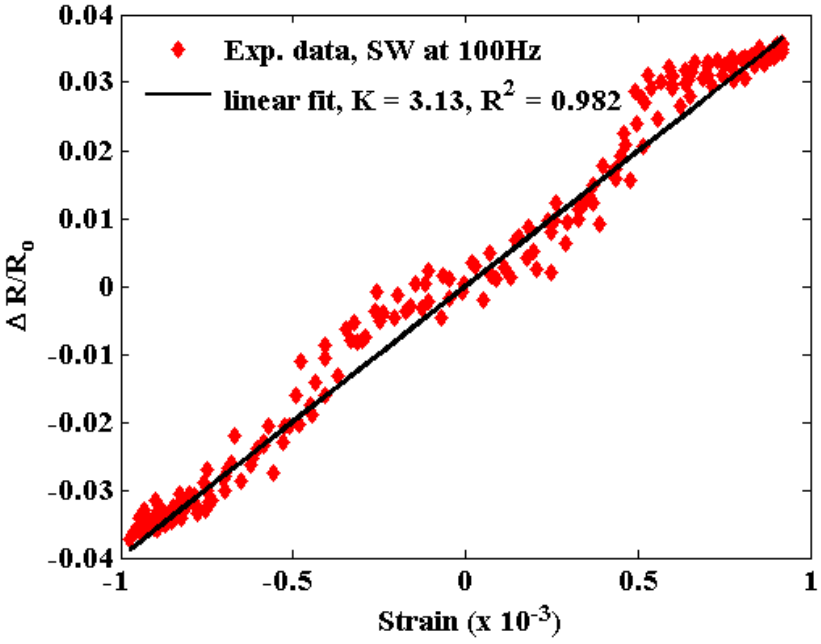
Exp. data, SW at 100Hz
linear fit, K = 3.13, R2 = 0.982
Δ R/R0
Strain (x 10-3)
0.04
0.03
0.02
0.01
0
-0.01
-0.02
-0.03
-0.04
-1
-0.5
0
0.5
1

Figure 10

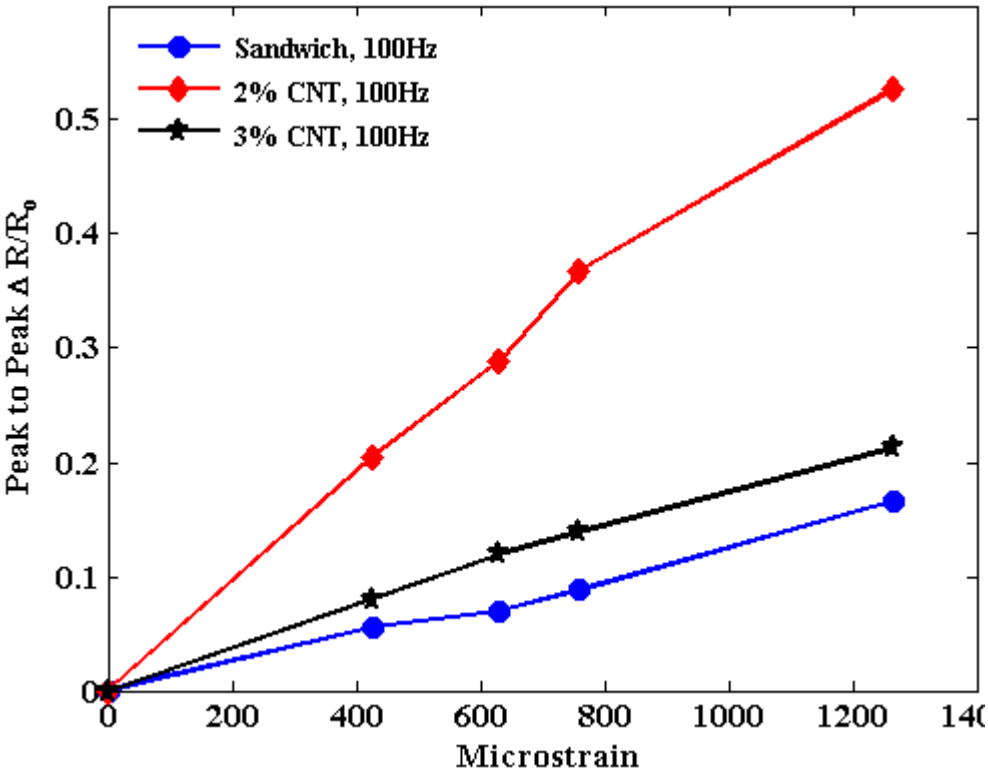
Sandwich, 100Hz
2% CNT, 100Hz
3% CNT, 100Hz
Peak to Peak Δ R/R0
0.5
0.4
0.3
0.2
0.1
0
0
200
400
600
800
1000
1200
Microstrain

Figure 11. (a)

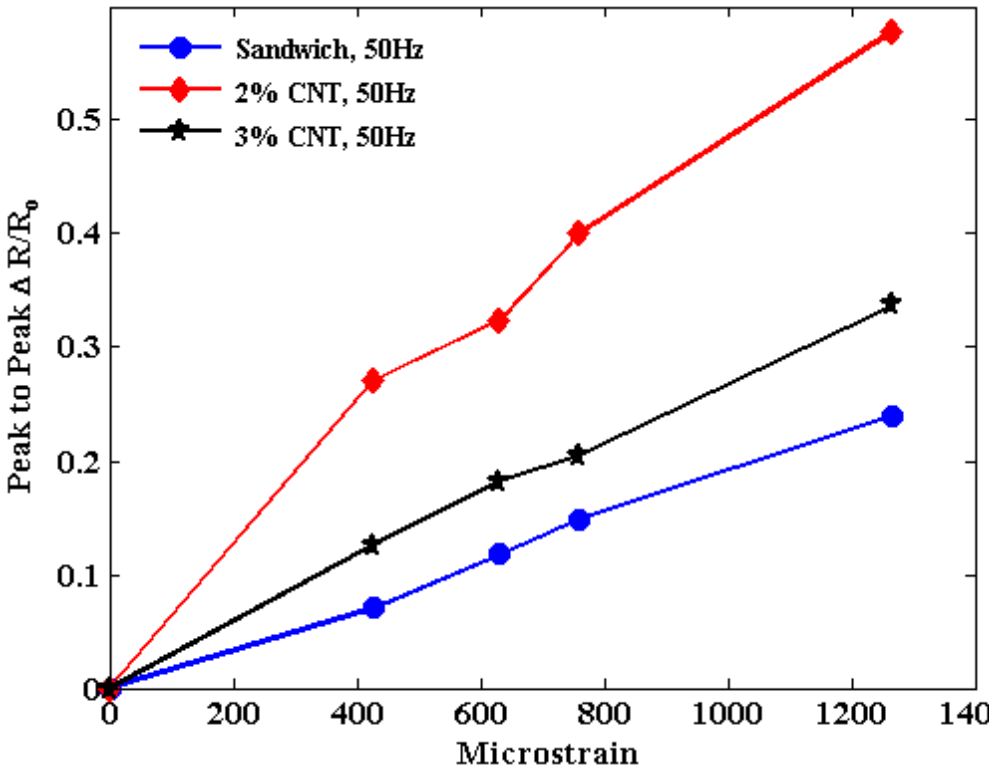
Sandwich, 50Hz
2% CNT, 50Hz
3% CNT, 50Hz
Peak to Peak Δ R/R0
0
0.1
0.2
0.3
0.4
0.5
0
200
400
600
800
1000
1200
140
Microstrain

Figure 11. (b)